Recurrent CNVs and SNVs at the *NPHP1* Locus Contribute Pathogenic Alleles to Bardet-Biedl Syndrome

Anna Lindstrand,[1,9] Erica E. Davis,[1] Claudia M.B. Carvalho,[2,3] Davut Pehlivan,[2] Jason R. Willer,[1] I-Chun Tsai,[1] Subhadra Ramanathan,[4] Craig Zuppan,[5] Aniko Sabo,[6] Donna Muzny,[6] Richard Gibbs,[6] Pengfei Liu,[2] Richard A. Lewis,[2] Eyal Banin,[7] James R. Lupski,[2,8] Robin Clark,[4] and Nicholas Katsanis[1,*]

Homozygosity for a recurrent 290 kb deletion of *NPHP1* is the most frequent cause of isolated nephronophthisis (NPHP) in humans. A deletion of the same genomic interval has also been detected in individuals with Joubert syndrome (JBTS), and in the mouse, *Nphp1* interacts genetically with *Ahi1*, a known JBTS locus. Given these observations, we investigated the contribution of *NPHP1* in Bardet-Biedl syndrome (BBS), a ciliopathy of intermediate severity. By using a combination of array-comparative genomic hybridization, *Taq*Man copy number assays, and sequencing, we studied 200 families affected by BBS. We report a homozygous *NPHP1* deletion CNV in a family with classical BBS that is transmitted with autosomal-recessive inheritance. Further, we identified heterozygous *NPHP1* deletions in two more unrelated persons with BBS who bear primary mutations at another BBS locus. In parallel, we identified five families harboring an SNV in *NPHP1* resulting in a conserved missense change, c.14G>T (p.Arg5Leu), that is enriched in our Hispanic pedigrees; in each case, affected individuals carried additional bona fide pathogenic alleles in another BBS gene. In vivo functional modeling in zebrafish embryos demonstrated that c.14G>T is a loss-of-function variant, and suppression of *nphp1* in concert with each of the primary BBS loci found in our *NPHP1*-positive pedigrees exacerbated the severity of the phenotype. These results suggest that *NPHP1* mutations are probably rare primary causes of BBS that contribute to the mutational burden of the disorder.

Nephrocystin-1 is a ciliary protein encoded by *NPHP1* on human chromosome 2q13 (MIM 607100; RefSeq accession number NM_000272.3; GI, 189491772). The genetic structure surrounding the gene and locus includes flanking 330 kb inverted low-copy repeats (LCR) that have 45 kb direct repeats embedded within them; this genomic architecture renders the locus susceptible to genomic instability mainly via nonallelic homologous recombination (NAHR).[1] A common 290 kb recurrent microdeletion with breakpoints located within the smaller direct repeats is present in approximately 1/400 normal individuals of northern European descent (estimated from the Database of Genomic Variants [DGV]). Homozygous deletions have never been detected in controls, suggesting that loss of *NPHP1* gives rise to penetrant pathology. However, the clinical expressivity of the homozygous deletion can be variable. In most cases reported, the deletion has been causally associated with isolated nephronophthisis (NPHP [MIM 256100])[1,2] or NPHP and retinal degeneration (Senior-Loken syndrome [SLS] [MIM 266900]);[3] however, rare deletion cases have also been identified with Joubert syndrome (JBTS [MIM 213300]), a severe ciliopathy hallmarked by developmental delay and central nervous system malformations.[4] Multiple in vivo and in vitro studies have demonstrated physical interaction, protein colocalization, and genetic interaction between NPHP1 and other ciliary proteins that include nephrocystin-3, nephrocystin-4, and inversin.[5–9] Moreover, a dosage-sensitive interaction between Nphp1 and Ahi1, for which the human ortholog is responsible for approximately 10% of JBTS,[10] has also been shown in rodent models; mice deficient for both proteins have a more severe retinal phenotype than do the single-gene knockouts.[11]

These observations prompted us to ask whether *NPHP1* harbors alleles that are contributory to other ciliopathies. To this end, we queried *NPHP1* mutations in a cohort of individuals with Bardet-Biedl syndrome (BBS [MIM 209900]), a rare (1:13,500–1:160,000) multisystemic ciliopathy characterized by retinal degeneration, obesity, polydactyly, mental retardation, renal dysfunction, and hypogonadism; BBS is also underscored by extensive genetic heterogeneity, allelic overlap with other ciliopathies, and both recessive and oligogenic forms of inheritance.[12–16]

First, we tested the copy-number status of *NPHP1* in 200 BBS-affected families (82.5% of individuals of European ancestry, 15% of Arab ancestry, 2.5% of Hispanic origin) and 229 control subjects of European descent. This analysis was part of a custom high-resolution oligonucleotide array comparative genomic hybridization (aCGH) scan of 772 genes prioritized from the ciliary proteome;[17] at the *NPHP1* locus, we placed 187 oligonucleotide probes,

[1]Center for Human Disease Modeling, Duke University School of Medicine, Durham, NC 27710, USA; [2]Department of Molecular and Human Genetics, Baylor College of Medicine, Houston, TX 77030, USA; [3]Centro de Pesquisas René Rachou – FIOCRUZ, Belo Horizonte, MG 30190-002, Brazil; [4]Division of Medical Genetics, Department of Pediatrics, Loma Linda University School of Medicine, Loma Linda, CA 92350, USA; [5]Pathology and Human Anatomy, Loma Linda University School of Medicine, Loma Linda, CA 92359, USA; [6]Human Genome Sequencing Center, Baylor College of Medicine, Houston, TX 77030, USA; [7]Center for Retinal and Macular Degenerations, Department of Ophthalmology, Hadassah-Hebrew University Medical Center, Jerusalem 91120, Israel; [8]Departments of Molecular and Human Genetics and Pediatrics, Baylor College of Medicine and Texas Children's Hospital, Houston, TX 77030, USA
[9]Present address: Department of Molecular Medicine & Surgery, Karolinska Institute, 17176 Stockholm, Sweden
*Correspondence: nicholas.katsanis@duke.edu
http://dx.doi.org/10.1016/j.ajhg.2014.03.017.

distributed across the intragenic coding and noncoding regions with an average resolution of 100 bp and 500 bp, respectively. The experiments were performed according to the manufacturer's recommendations with minor modifications via whole-genome amplified DNA in BBS cases and genomic DNA in controls.[18] Additional individuals from our pedigrees, as well as confirmatory analysis of candidate CNVs, were genotyped by *Taq*Man copy-number assays performed according to the manufacturer's recommendations. We used three different assays, located in exon 1 (Hs00036264_cn), exon 10 (Hs00095856_cn), and exon 20 (Hs00002984_cn) of *NPHP1* (RefSeq NM_000272.3; UCSC Genome Browser build hg19). Both the usage of human DNA samples and model organisms has been reviewed and approved by ethics board and animal care and use committees at Duke University. Informed consent was obtained before individuals were included in the study.

We identified three BBS-affected families in which the *NPHP1* recurrent deletion segregated with disease: one consanguineous Hispanic pedigree with a homozygous deletion (RC2), one consanguineous Israeli family with a heterozygous deletion (family 44), and one pedigree of northern European descent (AR704) also bearing a heterozygous deletion (Table 1, Figures 1 and 2). The deletion was not detected in any of our control samples. Moreover, to obtain a more accurate assessment of the frequency of the *NPHP1* deletion in the general population, and thus the power of the analysis, we combined our experimental control data with publicly available data from a genome-wide copy-number variant (CNV) screen by Itsara et al.[19] In this data set, heterozygous deletions were detected in 2/1,607 European controls.

Overall, we observed a deletion incidence of 1.5% of BBS-affected pedigrees (3/200). Although a rare event, data from the total BBS cohort versus the combined control data sets (our 229 controls plus the Itsara et al.[19] set) showed a significant enrichment of the *NPHP1* deletion allele in BBS ($p = 0.008$, Fisher's exact test). These data were likewise significant when compared to the entire DGV mixed population control data from 20,086 individuals ($p = 0.011$, chi-square with Yates correction). These findings suggest that the *NPHP1* deletion may contribute to BBS.

Next, we turned our attention to point mutations. We selected probands from 96 BBS-affected families without preselection for known mutations or CNVs, we PCR amplified all *NPHP1* (RefSeq NM_000272.3, hg19) coding exons and splice junctions, and we sequenced them according to standard Sanger methodology (primers and PCR conditions are available on request). We identified a single heterozygous variant that encoded a missense change, c.14G>T (p.Arg5Leu; rs190983114; RefSeq NM_000272.3; hg19), in three BBS-affected families (Table 1, Figure 2) of Hispanic (n = 2; RC1, AR888) or northern European (n = 1; DM012) origin. The variant position is evolutionarily invariant in all 39 species with a detectable *NPHP1* ortholog and is present in ultrarare frequencies in the Exome Variant Server database (EVS) (6/13,000 with an equal MAF of 0.04% in either European American [EA] or African American [AA] samples). To replicate this finding, we assessed the prevalence of the c.14G>T change in the second half of our BBS cohort by Sanger sequencing of *NPHP1* exon 1; we detected two additional BBS-affected families (AR082 and R1) that were heterozygous for the c.14G>T allele; both families were of Hispanic origin. Combined, we found that 2.5% of our overall cohort (5/200 families) carried the c.14G>T allele, which, similar to the deletion burden in our cohort, represents an apparent enrichment compared to controls.

We were struck by the fact that 4/5 of families with the c.14G>T allele were of Hispanic origin, a subset that is heavily underrepresented in our cohort, with only 14/200 families (n = 4/14 Hispanics with *NPHP1* c.14G>T; MAF 28%). This finding represents a significant enrichment of this allele compared to EA and AA controls (MAF < 0.04%). Given that EVS is bereft of Hispanic control data, and conscious of the fact that we might be observing a population-specific variant, we sequenced 277 control individuals of Hispanic origin; although the MAF of this allele was elevated in this population, the enrichment in our BBS cohort remained significant (28% versus 4.9% MAF%; $p = 0.04$; Fisher's exact test).

Our findings are reminiscent of the genetic architecture of other BBS and ciliopathy loci, in which low-frequency variants can contribute both causal and contributory alleles to the disease burden[13,20–26] but for which the genetic data alone suggest association but are insufficient to provide robust arguments for causality. We therefore turned to functional assays. We reasoned that (1) if *NPHP1* is relevant to BBS pathology, then suppression of the zebrafish ortholog of this gene should mimic the previously established phenotypes of *bbs* morphants at midsomitic stages[26,27] and also give rise to renal defects; and (2) if the c.14G>T allele is relevant to the function of the protein and the clinical phenotype of the affected individuals, this allele should fail to complement suppression of *nphp1* in vivo.

The *Danio rerio* genome has a single zebrafish *NPHP1* ortholog (*nphp1* [RefSeq NM_001077170]; 56% protein sequence identity with human NPHP1). We obtained a previously published *nphp1* translation-blocking (tb) morpholino (MO)[6] as well as a splice-blocking (sb) MO targeting the junction of *nphp1* exon 2/intron 2–3 (5′-ACA GATACAAGTCCTCTACCTCTGC-3′; Gene Tools). We injected progressively increasing sb-MO or tb-MO concentrations (3–9 ng, sb; 2–6 ng, tb) into wild-type (WT) zebrafish embryos at the 1–4 cell stage and we scored embryo clutches for shortened body axes, broader somites, and broad and kinked notochords at the 8–10 somite stage according to previously established objective criteria.[26] For each MO independently, we observed a dose-dependent increase in both the number of affected morphants and also the severity of the defects (Figure S1 available

Table 1. Detected Mutations and Clinical Findings in Affected Individuals with *NPHP1* Mutations

Subject; Origin	*NPHP1* Mutation (RefSeq NM_000272.3)	BBS Locus (Primary Causal Locus unless Indicated Otherwise)	Zebrafish Data[a]	RP	Polydactyly	Obesity	Hypogonadism	Renal Anomalies	Developmental Delay
RC2-03; Latino	*NPHP1*: del; hom	*BBS2*[b] (RefSeq NM_031885.3): c.367A>G (p.Ile123Val); hom	hypomorph	yes	yes	no	yes	nephronophthisis	yes
AR704-03; N. European	*NPHP1*: del; het	*BBS10*[c] (RefSeq NM_024685.3): c.145C>T (p.Arg49Trp); het	null	yes	yes	yes	NA	no	yes
AR704-04; N. European	*NPHP1*: del; het	*BBS10*[c] (RefSeq NM_024685.3): c.145C>T (p.Arg49Trp); het	null	yes	yes	yes	NA	no	yes
44/3; Israel	*NPHP1*: del; het	*BBS7* (RefSeq NM_176824.2): c.87_88delCA (p.His29Glnfs*12); hom	NA	yes	yes	yes	yes	born with one kidney; chronic renal failure; kidney transplantation	yes
44/4; Israel	*NPHP1*: del; het	*BBS7* (RefSeq NM_176824.2): c.87_88delCA (p.His29Glnfs*12); hom	NA	yes	yes	yes	NA	no	yes
AR888-03; Latino	*NPHP1*: c.14G>T (p.Arg5Leu); het	*BBS1* (RefSeq NM_024649.4): c.1645G>T (p.Glu549*); het	NA	yes	yes	yes	ND	impaired renal function; kidney cysts; enlarged kidney	yes
		BBS1[d] (RefSeq NM_024649.4): del exon1_11; het	NA						
RC1-03; Latino	*NPHP1*: c.14G>T (p.Arg5Leu); het	*BBS10* (RefSeq NM_024685.3): c.926T>C (p.Leu309Pro); het	ND	yes	yes	yes	yes	no	yes
		BBS10 (RefSeq NM_024685.3): c.9_14delTTCTAT (p.Ser3_Met5delinsArg); het	ND						
DM012-003; N. European	*NPHP1*: c.14G>T (p.Arg5Leu); het	*BBS10* (RefSeq NM_024685.3): c.271dupT (Cys91Leufs*5); hom	NA	yes	yes	yes	no	no	yes
R1-04; Latino	*NPHP1*: c.14G>T (p.Arg5Leu); het	*BBS9* (RefSeq NM_198428.2): c.1536A>G [p.(=)]; hom	ND	yes	ND	ND	ND	ND	ND
R1-05; Latino	*NPHP1*: c.14G>T (p.Arg5Leu); het	*BBS9* (RefSeq NM_198428.2): c.1536A>G [p.(=)]; hom		yes	ND	ND	ND	ND	ND
AR082-03; Latino	*NPHP1*: c.14G>T (p.Arg5Leu); het	*BBS9* (RefSeq NM_198428.2): c.1789C>T (p.Gln597*); hom	NA	yes	ND	ND	ND	ND	ND

Abbreviations are as follows: RP, retinitis pigmentosa; del, deletion; het, heterozygous; hom, homozygous; NA, not applicable (affected individual is female); ND, not determined.
[a]Data from Zaghloul et al.[26]
[b]Putative second-site modulator
[c]Heterozygous change, unclear whether causal locus
[d]Publicly available in dbVar (study ID: nstd93)

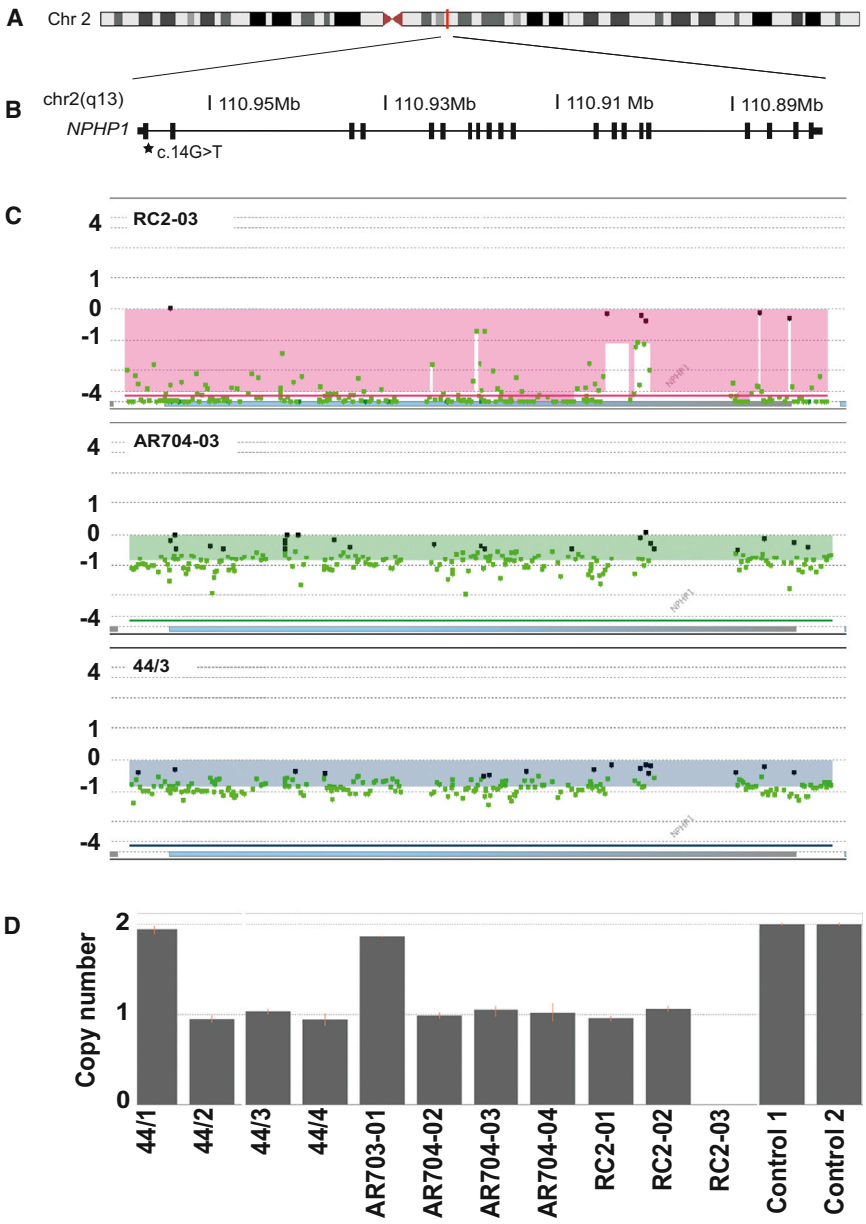

Figure 1. *NPHP1* Deletions in Individuals with BBS

(A) Schematic of human chromosome 2. A vertical red line indicates the position of *NPHP1* (RefSeq NM_000272.3) at 2q13.

(B) A zoomed depiction of the *NPHP1* locus with a schematic illustration of exons (vertical black bars). The genomic location on chromosome 2 (in Mb) is shown. c.14G>T (p.Arg5Leu) is indicated with a black star.

(C) High-resolution results from the aCGH analyses in individuals RC2-03 (top), AR704-03 (middle), and 44/3 (bottom) are visualized as a plot. The horizontal blue bar represents *NPHP1*. Individual dots represent specific oligonucleotide probes and are indicated as black (normal copy number), red (copy number gain), and green (copy number loss) compared to a reference sample. The normalized log2 ratios of the Cy5/Cy3 intensity values for cases versus controls are shown on the y axis.

(D) Segregation of the *NPHP1* deletion by *Taq*man copy number analysis using a probe (Hs00002984_cn) located within the *NPHP1* locus; individuals 44/2, 44/3, 44/4, AR704-02, AR704-03, AR704-04, RC2-01, and RC2-02 harbor a heterozygous deletion and RC2-03 has a homozygous deletion. Error bars were calculated by the CopyCaller Software and represent the copy number range of triplicate reactions.

online) that phenocopied the phenotypes observed in numerous ciliopathy morphants, including all tested BBS genes.[20,22,23,27–30] To test sb-MO efficiency, we harvested whole embryos in Trizol (Invitrogen) for total RNA extraction and reverse transcribed oligo-dT primed cDNA (Superscript III, Invitrogen) for PCR. An aberrant splicing product was detected in sb-MO-injected embryos (Figure S1).

To test for MO specificity, we coinjected MO with capped human WT *NPHP1* mRNA. In brief, to generate human *NPHP1* message, we cloned the full-length *NPHP1* open reading frame into the pCS2+ plasmid, linearized with NotI, and performed in vitro transcription with the SP6 mMessage mMachine kit (Ambion). Coinjection of 200 pg of WT human *NPHP1* mRNA with MO (3 ng sb-MO; 2 ng tb-MO) resulted in a significant rescue of morphant phenotypes (55% versus 39% abnormal for sb-MO versus sb-MO+WT; $p = 0.003$; Figure 3; $n = 60–62$ embryos/injection and 69% versus 45% abnormal for tb-MO versus tb-MO+WT; $p < 0.0001$; Figure S1; $n = 31–41$ embryos/injection). We then used the gastrulation phenotype to test the pathogenicity of the heterozygous c.14G>T *NPHP1* variant by comparing the ability of equivalent doses of *NPHP1* WT or c.14G>U mRNA to rescue the *nphp1* sb-MO-induced defects. Coinjection of *nphp1* sb-MO with human *NPHP1* mRNA harboring the c.14G>U mutation was significantly worse from embryo clutches injected with sb-MO coinjected with WT mRNA, suggesting that the mutation impedes NPHP1 function (Figures 3A and 3B). Injection of mutant *NPHP1* mRNA was indistinguishable from wild-type injection ($p = 0.79$), but injection of decreasing doses of c.14G>U mRNA alone resulted in a dose-dependent decrease of affected embryos (Figure S2), which indicates indirectly the decreased function conferred by the c.14G>T mutation.

In parallel, we tested two missense variants mined from EVS that had both a modest allele frequency (>1% MAF) and an apparent ethnicity-specific enrichment similar to c.14G>T (c.115C>A, rs33958626, MAF 0.6% in AA versus 4% in EA; and c.689C>T, rs113450177, MAF 3.3% AA versus 0% EA; RefSeq NM_000272.3; hg19). The efficiency

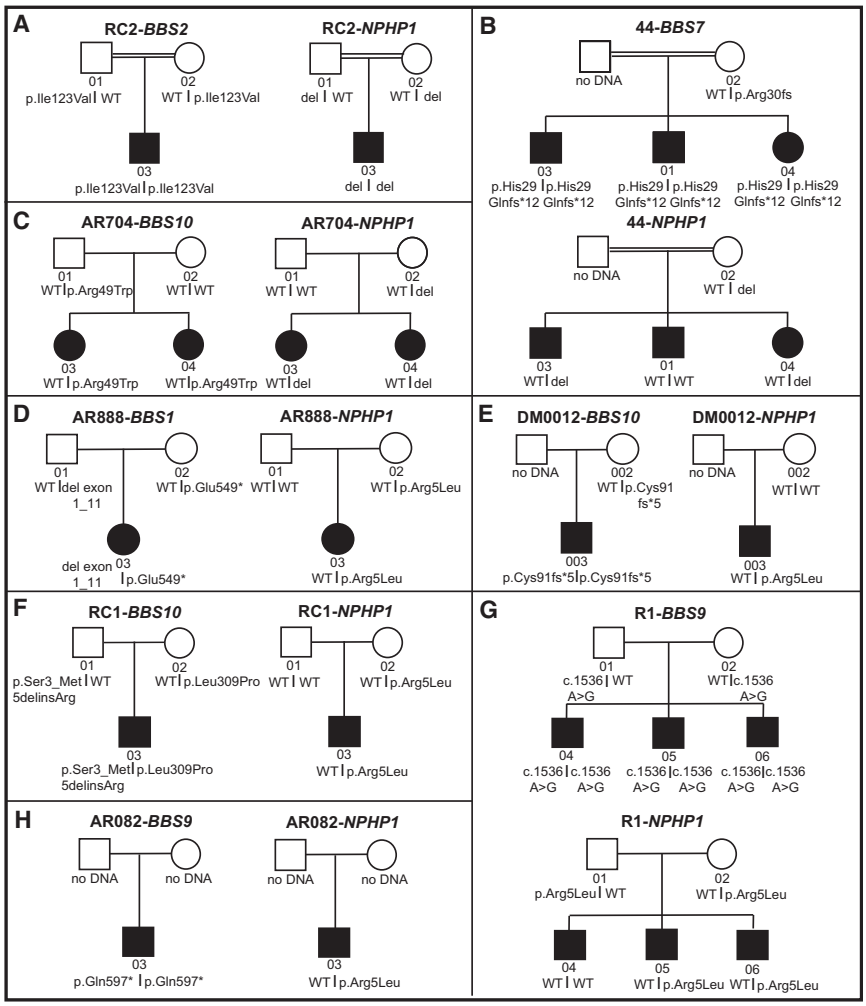

Figure 2. Pedigrees of the Families with *NPHP1* Mutations

Pedigrees and BBS gene mutational analysis results in all families with *NPHP1* mutations. Squares denote males and circles denote females. Blackened symbols represent the affected children and individual identification numbers are given below the symbols. Double lines indicate consanguinity.

of both variants to improve the *nphp1* MO gastrulation defects was not significantly different than that of WT mRNA, lending further evidence in favor of the specificity of the c.14G>T pathogenicity (Figure 3B, Table S1).

Next, we corroborated these findings in 4 day postfertilization (dpf) zebrafish larva by using a phenotypic readout directly relevant to NPHP. In brief, we reinjected sb-MO and/or mRNA at identical doses to those used for the gastrulation scoring and fixed embryos for whole-mount immunostaining with anti-NaK ATPase antibody (a6F, Developmental Studies Hybridoma Bank) as described.[31] Although we did not observe significant cyst formation in *nphp1* morphant batches (<1%), we did observe atrophy and diminished convolution of the proximal tubule, which is an orthologous renal feature consistent with NPHP in humans[32] (Figure 3C). Coinjection of sb-MO with WT mRNA improved significantly this defect (61% versus 30% affected for sb-MO versus WT+sb-MO, $p < 0.0001$, $n = 46$ embryos/injection with masked scoring), whereas embryo clutches injected with MO and c.14G>U mRNA were significantly worse than WT rescue (51% affected, $p < 0.0001$). These data corroborated our CE studies and suggested further that c.14G>T is pathogenic. Moreover, negative control variants c.115C>A and c.689C>T both scored benign in this assay, once again similar to the CE studies (Figures 3C and 3D; Table S1).

In aggregate, our data indicate that eight BBS-affected families bear loss-of-function mutations in *NPHP1* from either deletion CNVs or from a deleterious point mutation (SNV). We therefore asked (1) whether any of these alleles might be genetically necessary to drive the phenotype under a recessive paradigm and thus represent a Penetrant Mendelizing Variant (PMV); and (2) similar to other ciliopathy loci, whether the phenotype could be explained by the amalgam of mutations at multiple loci.

We first segregated all pathogenic variants in our families. In the family with the homozygous *NPHP1* deletion, segregation showed autosomal-recessive inheritance, with each of the parents being heterozygous carriers, as confirmed by a *Taq*man copy number assay (Figures 1D and 2A). By contrast, in the other two families with a heterozygous *NPHP1* deletion, there was no evidence of a second CNV in *NPHP1*, and sequencing of all exons was likewise negative for candidate pathogenic changes. These data suggested that this lesion might be coincidental in these families or be contributory to the genetic load of these pedigrees similar to what has been observed for other BBS loci.[13,14,20–26] We made similar observations for the five families bearing the c.14G>T allele, none of which carried additional *NPHP1* pathogenic alleles that were detectable within the constraints of our methodology.

Given these observations, and the fact that the BBS phenotype is more severe than what would be expected typically from a homozygous *NPHP1* deletion, we asked whether our *NPHP1*-positive pedigrees might bear additional pathogenic lesions in the known BBS loci; therefore, we performed Sanger-based sequencing analysis of the *BBS1-16* exons and splice junctions, which together account for ~75% of the disease burden in BBS.[15,33]

Consistent with the *NPHP1* deletion being the primary driver of BBS, sequencing of DNA from individuals in

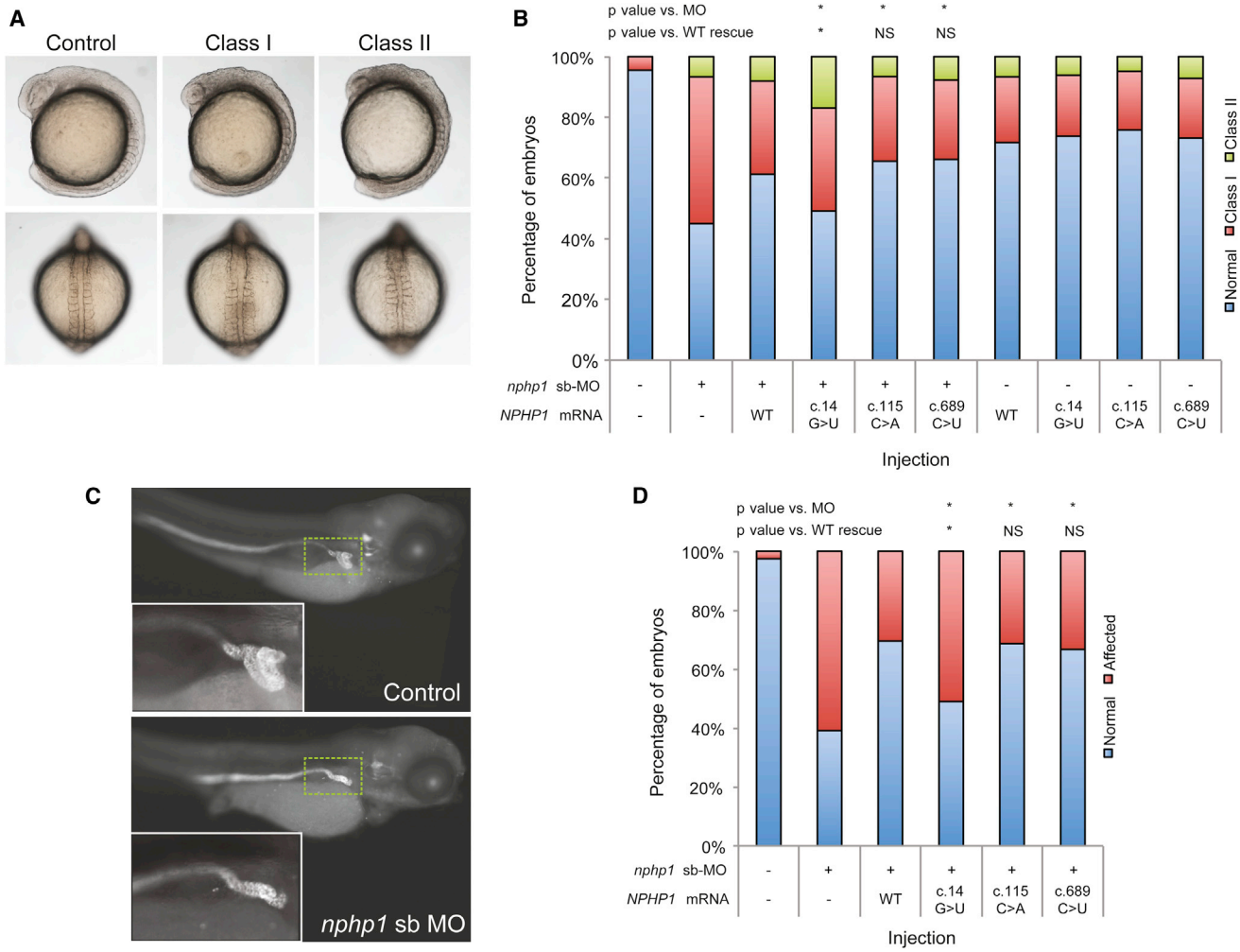

Figure 3. Morpholino-Induced Suppression of *nphp1* in Zebrafish Embryos Generates Gastrulation Defects and Abnormal Renal Morphology

(A) Live dorsal and lateral views of normal embryos and class I and class II morphants are shown. Live images of embryos were acquired on a Nikon AZ100 microscope at 8× magnification, with image capture facilitated by NIS Elements software (Nikon).

(B) Quantification of live scoring of *nphp1* MO and human mRNA (co)injections. Embryos were injected with the indicated dose (2 ng sb-MO and/or 200 pg *NPHP1* mRNA) and scored live according to criteria shown. n = 48–65 embryos/injection, repeated at least twice; with masked scoring; all comparisons were made using χ^2 tests; *p < 0.002; NS, not significant; see Table S1 for p values. c.115C>A (rs33958626) and c.689C>T (rs113450177) have similar minor allele frequencies (MAF; 4% in European Americans and 3.3% in African Americans) to that of c.14G>T (rs190983114) in our overall BBS cohort (2.5%), but result in rescue not significantly different from WT mRNA.

(C) Lateral views of representative larva fluorescently stained at 4 days postfertilization (dpf) with anti-NaK ATPase antibody (a6F, Developmental Studies Hybridoma Bank) to demarcate renal tubules. In comparison to controls, embryos injected with *nphp1* sb-MO have atrophy and reduced convolution of the proximal tubule. Inset area indicated by dashed green line.

(D) Quantification of renal phenotyping of *nphp1* MO and human mRNA (co)injections. Embryos were injected with the indicated dose (2 ng sb-MO and/or 200 pg *NPHP1* mRNA) and immunostained with anti-NaK ATPase antibody and scored as normal or affected (as shown in panel C), n = 46–51 embryos/injection, repeated at least twice; with masked scoring; all comparisons were made with χ^2 tests; *p < 0.05; NS, not significant; see Table S1 for p values.

family RC2 yielded no biallelic mutations under a recessive model. These data, together with the fact that the *NPHP1* deletion has never been observed in homozygosity in control individuals, indicates that this lesion is the most likely primary driver of the disease in the family, or PMV, potentially defining a new BBS locus. Consistent with this notion, phenotypic analysis of the affected individual (RC2-03) that included a renal biopsy indicated that the proband, in addition to his classical BBS features (retinal degeneration, polydactyly, developmental delay, hypogonadism), was notable for tubular interstitial and glomerular injury, findings uncommon in BBS[34] but typical of nephronophthisis (Figure 4).

Of note, individual RC2-03 harbors a homozygous *BBS2* variant, c.367A>G (p.Ile123Val). This allele cannot be causal to BBS, because it is present in homozygosity in ~4% of EA and 8% of Hispanic control subjects (rs11373; dbSNP; RefSeq NM_031885.3; hg19). However, this

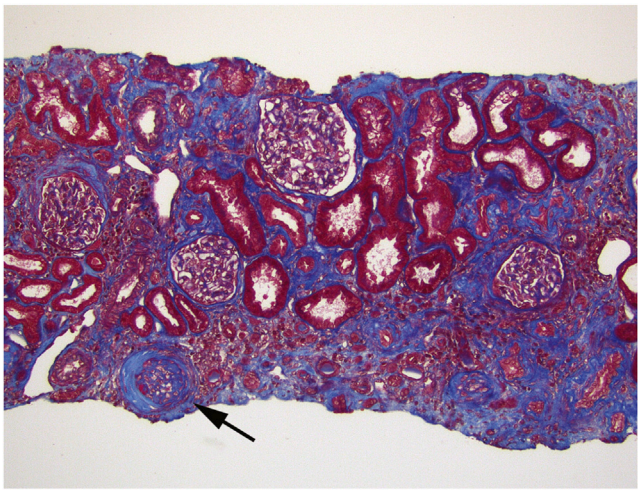

Figure 4. Renal Biopsy on Individual RC2-03
Renal biopsy on RC2-03, showing moderate tubular atrophy and interstitial fibrosis, with one obsolescent glomerulus (arrow). In the context of this individual, the findings are consistent with juvenile nephronophthisis. (Trichrome stain, original magnification ×100.)

change has been shown previously to be a functional hypomorph that is enriched significantly and overtransmitted in individuals with BBS,[26] raising the possibility that *NPHP1* and *BBS2* might interact genetically.

We similarly analyzed the coding regions of *BBS1-16*[16] by Sanger sequencing in the other seven families. In five of them, we identified a primary BBS driver locus. In the other two families (AR888 and AR704), we evaluated *BBS1* and *BBS10*, respectively, for CNVs that could unmask the second recessive allele. We identified a paternally inherited 17.7 kb deletion of *BBS1* (RefSeq NM_024649.4; hg19) exons 1–11 (in AR888 in *trans* with a truncating point mutation), thereby adding a sixth pedigree with a characterized primary driver locus (Table 1, Figures 2 and S3). The causal locus in AR704 remains unclear; we cannot rule out the possibility that AR704 harbors a second *BBS10* allele in a regulatory region, or that *BBS10* functions as a second-site modulator to a hitherto unidentified BBS gene.

Together, our CNV and sequencing data showed one pedigree in which homozygous loss of *NPHP1* is coincident with a homozygous hypomorph in *BBS2*; in the remaining families, heterozygous *NPHP1* loss-of-function alleles are coinherited with mutations in each of *BBS1*, *BBS7*, *BBS9*, and *BBS10*. We note that these predominant causal loci in the NPHP1-mutation-bearing pedigrees differ somewhat from the reported relative contributions of BBS genes to the disorder,[15,33] which may either be a chance event or may be suggestive of a unique biochemical relationship between NPHP1 and these BBS proteins.

As a first step toward investigating these possibilities, we asked whether genetic interaction between *NPHP1* and the primary BBS driver loci can exacerbate the severity of disease in a manner reminiscent of the reported *NPHP1-AHI1* interaction,[11] as well as the interaction reported previously for various binary combinations of ciliopathy[13,20,22–26,35–38] and nonciliopathy[21] loci. We therefore coinjected subeffective doses of the *nphp1* sb-MO (0.5 ng) with each of *bbs1* (3 ng), *bbs2* (1 ng), *bbs7* (3.5 ng), *bbs9* (2 ng), and *bbs10* (4 ng)[26] (Figure 5, Table S1). In each pairwise combination, gastrulation phenotypes were significantly more severe in the double MO injected embryos compared to the single MO injections alone (n = 61–255 embryos/injection; masked scoring). Similarly, the presence of proximal renal tubule atrophy in 4 dpf larva showed that for each pairwise combination, renal phenotypes were exacerbated significantly in comparison to single MO injections alone (n = 16–95 embryos/injection; masked scoring). Together, these data indicate that suppression of NPHP1 activity, in combination with loss of function of any tested BBS locus, can interact to exacerbate phenotypic severity. We do not have the resolution to determine whether these effects are additive or multiplicative, although our functional studies are more consistent with an additive model.

Given that we discovered a single BBS-affected family with recessive *NPHP1* deletions, it will be necessary to identify additional individuals who fulfill BBS clinical criteria but have causal molecular lesions at the *NPHP1* locus. Browsing the Database of Chromosome Imbalance and Phenotype in Humans using Ensembl Resources (DECIPHER) identified one additional case with the homozygous *NPHP1* deletion. The phenotypic information available (oculomotor apraxia; delayed speech and language development; intellectual disability) partially overlaps with BBS (but also with JBTS) but only for neurocognitive features that are typical triggers for ordering clinical aCGH testing. However, our data potentially extend the phenotypic spectrum of *NPHP1* loss of function, wherein homozygous deletion of the locus can give rise to ciliopathy phenotypes in the intermediate continuum between classical isolated NPHP and the severe JBTS phenotype. These data predict that individuals affected by other ciliopathies might also bear similar lesions and suggest that extending the diagnostic analysis of ciliary disease cases to include this *NPHP1* CNV, and potential CNVs at other ciliopathy loci,[17] might inform further the genetics of ciliopathies and other complex traits.

More broadly, our data also suggest that *NPHP1* mirrors other ciliopathy loci, contributing both causal and/or contributory alleles to the genetic burden of the disease. The observed deletion removes *NPHP1* and a fragment of the neighboring gene *MALL*; however, previous studies have detected the heterozygous deletion in *trans* with a coding change in *NPHP1* in persons with NPHP, but they did not detect mutations in *MALL*.[2] As such, although we cannot formally exclude the contribution of *MALL* to BBS, we consider that unlikely.

Our observations, together with previous studies, suggest that the *NPHP1* lesion might not be deterministic for

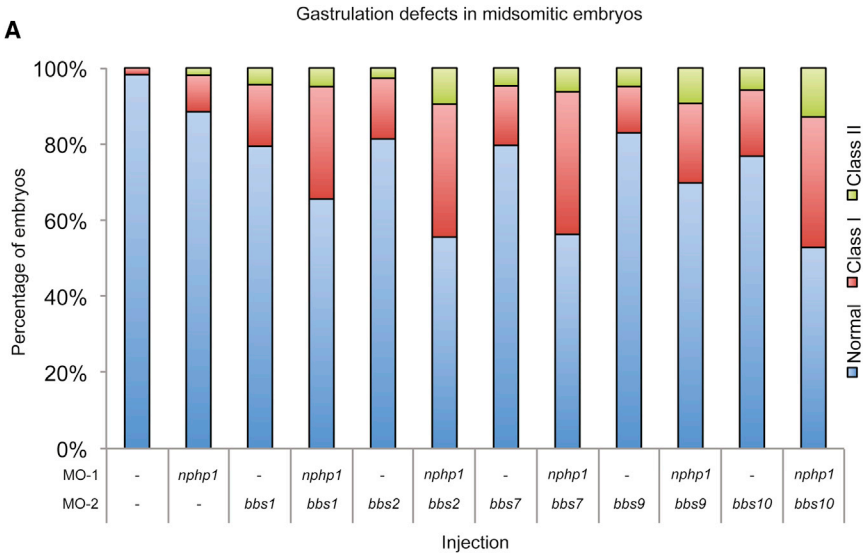

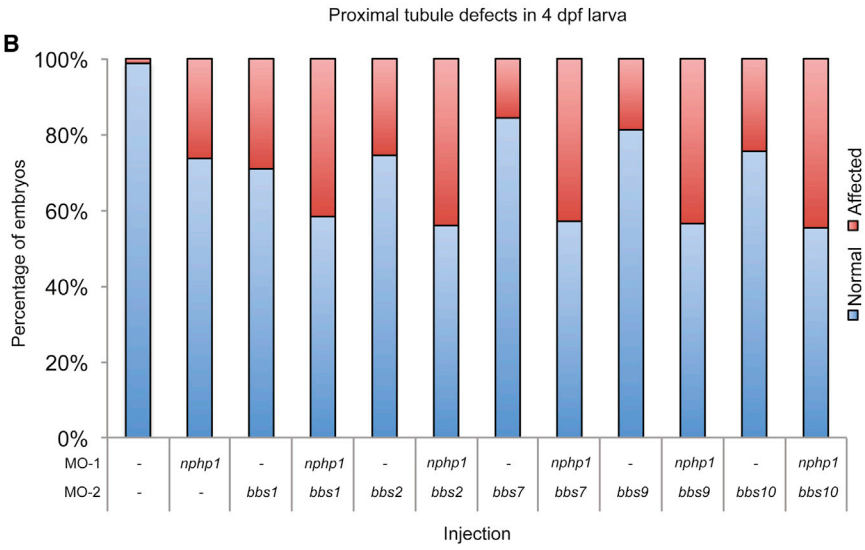

Figure 5. *nphp1* Interacts Genetically with All Primary BBS Loci Identified in BBS Cases with *NPHP1* Mutations

(A) Gastrulation defects in midsomitic embryos. Coinjection of a subeffective dose of *nphp1* sb-MO together with each of *bbs1*, *bbs2*, *bbs7*, *bbs9*, and *bbs10* MOs significantly increase the gastrulation phenotype compared to the same dose injected alone. n = 61–255 embryos/injection, 0.5 ng of *nphp1* sb-MO, 3 ng of *bbs1*-MO, 1 ng of *bbs2*-MO, 3.5 ng of *bbs7*-MO, 2 ng of *bbs9*-MO, and 4 ng of *bbs10*-MO was used, scoring as in Figure 3A.

(B) Proximal tubule defects in 4 dpf larva. Coinjection of a subeffective dose of *nphp1* sb-MO together with each of the five *bbs* MOs (same doses as in A) increase significantly the renal phenotype at 4 dpf compared to the same dose injected alone. n = 16–95 embryos/injection, scoring as in Figure 3B. See Table S1 for p values.

renal disease. First, mouse breeding experiments have shown that the *Nphp1-Ahi1* interaction can exacerbate retinal pathology.[11] Second, although the individual (RC2-03) with the homozygous *NPHP1* deletion does manifest hallmarks of NPHP-like renal pathology, only two of our other ten BBS-affected individuals with heterozygous *NPHP1* lesions had renal defects. This is not surprising, given that we interrogated only a small fraction of the ciliary proteome (or the genome) and that, as emerging data suggest, the primary cilium is sensitive to *trans*-epistasis that can either exacerbate or ameliorate the phenotype, as exemplified by the protective effect of loss-of-function *Bbs6* mutations on *Cep290* and the likewise protective effect of loss-of-function axonemal mutations on a genetic background sensitized by PKD mutations in mice.[36,38]

In the present work, the challenges of interpreting the contribution of heterozygous rare alleles in the context of primary causal lesions are exacerbated by the identification of alleles with ethnic-specific enrichment. The c.14G>T allele is ultrarare in northern European and African American control subjects (MAF < 0.04%) but is elevated in Hispanics, a population that has been undersampled for BBS. In these instances, statistical arguments alone remain constrained by the availability of cases and appropriate controls. Thus, the synthesis of population data with rigorous functional studies of allele effect may aid interpretation of the potential functional consequences of the burden of rare alleles and their impact on the penetrance and expression of the disease in an ethnicity-specific manner.[39]

Supplemental Data

Supplemental Data include three figures and one table and can be found with this article online at http://dx.doi.org/10.1016/j.ajhg.2014.03.017.

Acknowledgments

We are grateful to the BBS-affected families for their continued enthusiasm in our work. We thank John Belmont at Baylor College of Medicine and Shelby Strickland, Yutao Liu, Rand Allingham, and Michael Hauser at Duke University for Hispanic control DNAs. This work was funded by NIH grants DK072301, DK075972-09, and HD042601 to N.K., NS058529 to J.R.L., and EY021872 to E.E.D. and F32DK094578 to I.-C. T.; by funding from EU 7th FP under GA nr. 241955, project SYSCILIA to N.K.

and E.E.D.; and by the Swedish Research Council grant 2010-978 to A.L. N.K. is a distinguished Jean and George Brumley Professor.

Received: August 19, 2013
Accepted: March 25, 2014
Published: April 17, 2014

Web Resources

The URLs for data presented herein are as follows:

Database of Genomic Variants (DGV), http://dgv.tcag.ca/dgv/app/home
dbVar, http://www.ncbi.nlm.nih.gov/dbvar/
DECIPHER, http://decipher.sanger.ac.uk/
Ensembl Genome Browser, http://www.ensembl.org/index.html
NCBI, http://www.ncbi.nlm.nih.gov/
NHLBI Exome Sequencing Project (ESP) Exome Variant Server, http://evs.gs.washington.edu/EVS/
Online Mendelian Inheritance in Man (OMIM), http://www.omim.org/
RefSeq, http://www.ncbi.nlm.nih.gov/RefSeq
UCSC Genome Browser, http://genome.ucsc.edu

Accession Numbers

The dbVar accession number for the study that identified the *BBS1* copy-number variant reported in this paper is nstd93.

References

1. Saunier, S., Calado, J., Benessy, F., Silbermann, F., Heilig, R., Weissenbach, J., and Antignac, C. (2000). Characterization of the NPHP1 locus: mutational mechanism involved in deletions in familial juvenile nephronophthisis. Am. J. Hum. Genet. *66*, 778–789.
2. Hildebrandt, F., Otto, E., Rensing, C., Nothwang, H.G., Vollmer, M., Adolphs, J., Hanusch, H., and Brandis, M. (1997). A novel gene encoding an SH3 domain protein is mutated in nephronophthisis type 1. Nat. Genet. *17*, 149–153.
3. Caridi, G., Murer, L., Bellantuono, R., Sorino, P., Caringella, D.A., Gusmano, R., and Ghiggeri, G.M. (1998). Renal-retinal syndromes: association of retinal anomalies and recessive nephronophthisis in patients with homozygous deletion of the NPH1 locus. Am. J. Kidney Dis. *32*, 1059–1062.
4. Parisi, M.A., Bennett, C.L., Eckert, M.L., Dobyns, W.B., Gleeson, J.G., Shaw, D.W., McDonald, R., Eddy, A., Chance, P.F., and Glass, I.A. (2004). The NPHP1 gene deletion associated with juvenile nephronophthisis is present in a subset of individuals with Joubert syndrome. Am. J. Hum. Genet. *75*, 82–91.
5. Delous, M., Hellman, N.E., Gaudé, H.M., Silbermann, F., Le Bivic, A., Salomon, R., Antignac, C., and Saunier, S. (2009). Nephrocystin-1 and nephrocystin-4 are required for epithelial morphogenesis and associate with PALS1/PATJ and Par6. Hum. Mol. Genet. *18*, 4711–4723.
6. Slanchev, K., Pütz, M., Schmitt, A., Kramer-Zucker, A., and Walz, G. (2011). Nephrocystin-4 is required for pronephric duct-dependent cloaca formation in zebrafish. Hum. Mol. Genet. *20*, 3119–3128.
7. Otto, E.A., Schermer, B., Obara, T., O'Toole, J.F., Hiller, K.S., Mueller, A.M., Ruf, R.G., Hoefele, J., Beekmann, F., Landau, D., et al. (2003). Mutations in INVS encoding inversin cause nephronophthisis type 2, linking renal cystic disease to the function of primary cilia and left-right axis determination. Nat. Genet. *34*, 413–420.
8. Mollet, G., Salomon, R., Gribouval, O., Silbermann, F., Bacq, D., Landthaler, G., Milford, D., Nayir, A., Rizzoni, G., Antignac, C., and Saunier, S. (2002). The gene mutated in juvenile nephronophthisis type 4 encodes a novel protein that interacts with nephrocystin. Nat. Genet. *32*, 300–305.
9. Olbrich, H., Fliegauf, M., Hoefele, J., Kispert, A., Otto, E., Volz, A., Wolf, M.T., Sasmaz, G., Trauer, U., Reinhardt, R., et al. (2003). Mutations in a novel gene, NPHP3, cause adolescent nephronophthisis, tapeto-retinal degeneration and hepatic fibrosis. Nat. Genet. *34*, 455–459.
10. Ferland, R.J., Eyaid, W., Collura, R.V., Tully, L.D., Hill, R.S., Al-Nouri, D., Al-Rumayyan, A., Topcu, M., Gascon, G., Bodell, A., et al. (2004). Abnormal cerebellar development and axonal decussation due to mutations in AHI1 in Joubert syndrome. Nat. Genet. *36*, 1008–1013.
11. Louie, C.M., Caridi, G., Lopes, V.S., Brancati, F., Kispert, A., Lancaster, M.A., Schlossman, A.M., Otto, E.A., Leitges, M., Gröne, H.J., et al. (2010). AHI1 is required for photoreceptor outer segment development and is a modifier for retinal degeneration in nephronophthisis. Nat. Genet. *42*, 175–180.
12. Badano, J.L., Kim, J.C., Hoskins, B.E., Lewis, R.A., Ansley, S.J., Cutler, D.J., Castellan, C., Beales, P.L., Leroux, M.R., and Katsanis, N. (2003). Heterozygous mutations in BBS1, BBS2 and BBS6 have a potential epistatic effect on Bardet-Biedl patients with two mutations at a second BBS locus. Hum. Mol. Genet. *12*, 1651–1659.
13. Badano, J.L., Leitch, C.C., Ansley, S.J., May-Simera, H., Lawson, S., Lewis, R.A., Beales, P.L., Dietz, H.C., Fisher, S., and Katsanis, N. (2006). Dissection of epistasis in oligogenic Bardet-Biedl syndrome. Nature *439*, 326–330.
14. Katsanis, N., Ansley, S.J., Badano, J.L., Eichers, E.R., Lewis, R.A., Hoskins, B.E., Scambler, P.J., Davidson, W.S., Beales, P.L., and Lupski, J.R. (2001). Triallelic inheritance in Bardet-Biedl syndrome, a Mendelian recessive disorder. Science *293*, 2256–2259.
15. Zaghloul, N.A., and Katsanis, N. (2009). Mechanistic insights into Bardet-Biedl syndrome, a model ciliopathy. J. Clin. Invest. *119*, 428–437.
16. Davis, E.E., and Katsanis, N. (2012). The ciliopathies: a transitional model into systems biology of human genetic disease. Curr. Opin. Genet. Dev. *22*, 290–303.
17. Hjeij, R., Lindstrand, A., Francis, R., Zariwala, M.A., Liu, X., Li, Y., Damerla, R., Dougherty, G.W., Abouhamed, M., Olbrich, H., et al. (2013). ARMC4 mutations cause primary ciliary dyskinesia with randomization of left/right body asymmetry. Am. J. Hum. Genet. *93*, 357–367.
18. Carvalho, C.M., Zhang, F., Liu, P., Patel, A., Sahoo, T., Bacino, C.A., Shaw, C., Peacock, S., Pursley, A., Tavyev, Y.J., et al. (2009). Complex rearrangements in patients with duplications of MECP2 can occur by fork stalling and template switching. Hum. Mol. Genet. *18*, 2188–2203.
19. Itsara, A., Cooper, G.M., Baker, C., Girirajan, S., Li, J., Absher, D., Krauss, R.M., Myers, R.M., Ridker, P.M., Chasman, D.I., et al. (2009). Population analysis of large copy number variants and hotspots of human genetic disease. Am. J. Hum. Genet. *84*, 148–161.
20. Davis, E.E., Zhang, Q., Liu, Q., Diplas, B.H., Davey, L.M., Hartley, J., Stoetzel, C., Szymanska, K., Ramaswami, G., Logan,

C.V., et al.; NISC Comparative Sequencing Program (2011). TTC21B contributes both causal and modifying alleles across the ciliopathy spectrum. Nat. Genet. *43*, 189–196.
21. de Pontual, L., Zaghloul, N.A., Thomas, S., Davis, E.E., McGaughey, D.M., Dollfus, H., Baumann, C., Bessling, S.L., Babarit, C., Pelet, A., et al. (2009). Epistasis between RET and BBS mutations modulates enteric innervation and causes syndromic Hirschsprung disease. Proc. Natl. Acad. Sci. USA *106*, 13921–13926.
22. Khanna, H., Davis, E.E., Murga-Zamalloa, C.A., Estrada-Cuzcano, A., Lopez, I., den Hollander, A.I., Zonneveld, M.N., Othman, M.I., Waseem, N., Chakarova, C.F., et al. (2009). A common allele in RPGRIP1L is a modifier of retinal degeneration in ciliopathies. Nat. Genet. *41*, 739–745.
23. Leitch, C.C., Zaghloul, N.A., Davis, E.E., Stoetzel, C., Diaz-Font, A., Rix, S., Alfadhel, M., Lewis, R.A., Eyaid, W., Banin, E., et al. (2008). Hypomorphic mutations in syndromic encephalocele genes are associated with Bardet-Biedl syndrome. Nat. Genet. *40*, 443–448.
24. Putoux, A., Thomas, S., Coene, K.L., Davis, E.E., Alanay, Y., Ogur, G., Uz, E., Buzas, D., Gomes, C., Patrier, S., et al. (2011). KIF7 mutations cause fetal hydrolethalus and acrocallosal syndromes. Nat. Genet. *43*, 601–606.
25. Stoetzel, C., Laurier, V., Davis, E.E., Muller, J., Rix, S., Badano, J.L., Leitch, C.C., Salem, N., Chouery, E., Corbani, S., et al. (2006). BBS10 encodes a vertebrate-specific chaperonin-like protein and is a major BBS locus. Nat. Genet. *38*, 521–524.
26. Zaghloul, N.A., Liu, Y., Gerdes, J.M., Gascue, C., Oh, E.C., Leitch, C.C., Bromberg, Y., Binkley, J., Leibel, R.L., Sidow, A., et al. (2010). Functional analyses of variants reveal a significant role for dominant negative and common alleles in oligogenic Bardet-Biedl syndrome. Proc. Natl. Acad. Sci. USA *107*, 10602–10607.
27. Gerdes, J.M., Liu, Y., Zaghloul, N.A., Leitch, C.C., Lawson, S.S., Kato, M., Beachy, P.A., Beales, P.L., DeMartino, G.N., Fisher, S., et al. (2007). Disruption of the basal body compromises proteasomal function and perturbs intracellular Wnt response. Nat. Genet. *39*, 1350–1360.
28. Li, C., Inglis, P.N., Leitch, C.C., Efimenko, E., Zaghloul, N.A., Mok, C.A., Davis, E.E., Bialas, N.J., Healey, M.P., Héon, E., et al. (2008). An essential role for DYF-11/MIP-T3 in assembling functional intraflagellar transport complexes. PLoS Genet. *4*, e1000044.
29. Valente, E.M., Logan, C.V., Mougou-Zerelli, S., Lee, J.H., Silhavy, J.L., Brancati, F., Iannicelli, M., Travaglini, L., Romani, S., Illi, B., et al. (2010). Mutations in TMEM216 perturb ciliogenesis and cause Joubert, Meckel and related syndromes. Nat. Genet. *42*, 619–625.
30. McIntyre, J.C., Davis, E.E., Joiner, A., Williams, C.L., Tsai, I.C., Jenkins, P.M., McEwen, D.P., Zhang, L., Escobado, J., Thomas, S., et al.; NISC Comparative Sequencing Program (2012). Gene therapy rescues cilia defects and restores olfactory function in a mammalian ciliopathy model. Nat. Med. *18*, 1423–1428.
31. Drummond, I.A., and Davidson, A.J. (2010). Zebrafish kidney development. Methods Cell Biol. *100*, 233–260.
32. Hildebrandt, F., Attanasio, M., and Otto, E. (2009). Nephronophthisis: disease mechanisms of a ciliopathy. J. Am. Soc. Nephrol. *20*, 23–35.
33. Redin, C., Le Gras, S., Mhamdi, O., Geoffroy, V., Stoetzel, C., Vincent, M.C., Chiurazzi, P., Lacombe, D., Ouertani, I., Petit, F., et al. (2012). Targeted high-throughput sequencing for diagnosis of genetically heterogeneous diseases: efficient mutation detection in Bardet-Biedl and Alström syndromes. J. Med. Genet. *49*, 502–512.
34. Beales, P.L., Elcioglu, N., Woolf, A.S., Parker, D., and Flinter, F.A. (1999). New criteria for improved diagnosis of Bardet-Biedl syndrome: results of a population survey. J. Med. Genet. *36*, 437–446.
35. Huang, L., Szymanska, K., Jensen, V.L., Janecke, A.R., Innes, A.M., Davis, E.E., Frosk, P., Li, C., Willer, J.R., Chodirker, B.N., et al. (2011). TMEM237 is mutated in individuals with a Joubert syndrome related disorder and expands the role of the TMEM family at the ciliary transition zone. Am. J. Hum. Genet. *89*, 713–730.
36. Ma, M., Tian, X., Igarashi, P., Pazour, G.J., and Somlo, S. (2013). Loss of cilia suppresses cyst growth in genetic models of autosomal dominant polycystic kidney disease. Nat. Genet. *45*, 1004–1012.
37. O'Toole, J.F., Liu, Y., Davis, E.E., Westlake, C.J., Attanasio, M., Otto, E.A., Seelow, D., Nurnberg, G., Becker, C., Nuutinen, M., et al. (2010). Individuals with mutations in XPNPEP3, which encodes a mitochondrial protein, develop a nephronophthisis-like nephropathy. J. Clin. Invest. *120*, 791–802.
38. Rachel, R.A., May-Simera, H.L., Veleri, S., Gotoh, N., Choi, B.Y., Murga-Zamalloa, C., McIntyre, J.C., Marek, J., Lopez, I., Hackett, A.N., et al. (2012). Combining Cep290 and Mkks ciliopathy alleles in mice rescues sensory defects and restores ciliogenesis. J. Clin. Invest. *122*, 1233–1245.
39. Wiszniewski, W., Hunter, J.V., Hanchard, N.A., Willer, J.R., Shaw, C., Tian, Q., Illner, A., Wang, X., Cheung, S.W., Patel, A., et al. (2013). TM4SF20 ancestral deletion and susceptibility to a pediatric disorder of early language delay and cerebral white matter hyperintensities. Am. J. Hum. Genet. *93*, 197–210.

The American Journal of Human Genetics, Volume *94*

Supplemental Data

Recurrent CNVs and SNVs at the *NPHP1* Locus Contribute Pathogenic Alleles to Bardet-Biedl Syndrome

Anna Lindstrand, Erica E. Davis, Claudia M.B. Carvalho, Davut Pehlivan, Jason R. Willer, I-Chun Tsai, Subhadra Ramanathan, Craig Zuppan, Aniko Sabo, Donna Muzny, Richard Gibbs, Pengfei Liu, Richard A. Lewis, Eyal Banin, James R. Lupski, Robin Clark, and Nicholas Katsanis

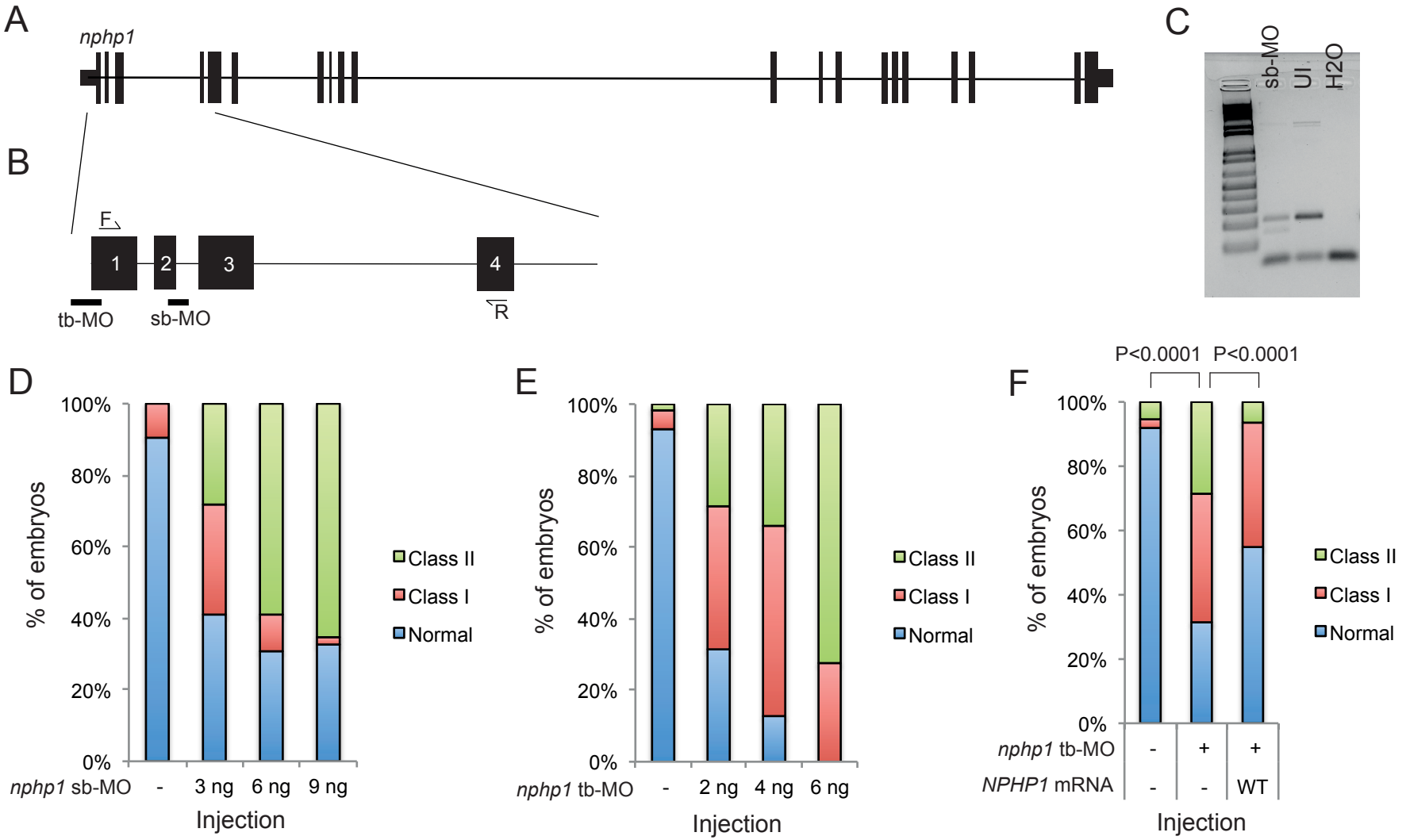

Figure S1: Knockdown efficiency of the *nphp1* morpholinos in zebrafish embryos

(A) Schematic illustration of the *D. rerio nphp1* (NM_001077170.1) locus.

(B) A zoomed schematic of exon 1 through exon 4 illustrating the position of the translational blocking (tb) and splice blocking (sb) MOs and RT-PCR primer target location. Total RNA was extracted from 10-somite stage embryos injected with 3ng of *nphp1* sb-MO (targeting exon2/intron2-3). After cDNA synthesis RT-PCR was performed with primers flanking the sb-MO target sites (F and R).

(C) Aberrant splicing was clearly visible by agarose gel electrophoresis following PCR amplification.

(D) Dose response curve for *nphp1* sb-MO. Wild type zebrafish embryos were injected at the 1 to 4 cell stage with the indicated dose. Embryos were kept at 23° C and scored live for gastrulation defects 24h post fertilization, mutant embryos were subdivided into class I or class II depending on the severity of the phenotype.

(E) Dose response curve for *nphp1* tb-MO as in (D).

(F) Co-injections of *nphp1* tb-MO with wild type (WT) human *NPHP1* mRNA result in a significant decrease in the number of morphant class I and class II embryos compared to tb-MO injected batches (P<0.0001).

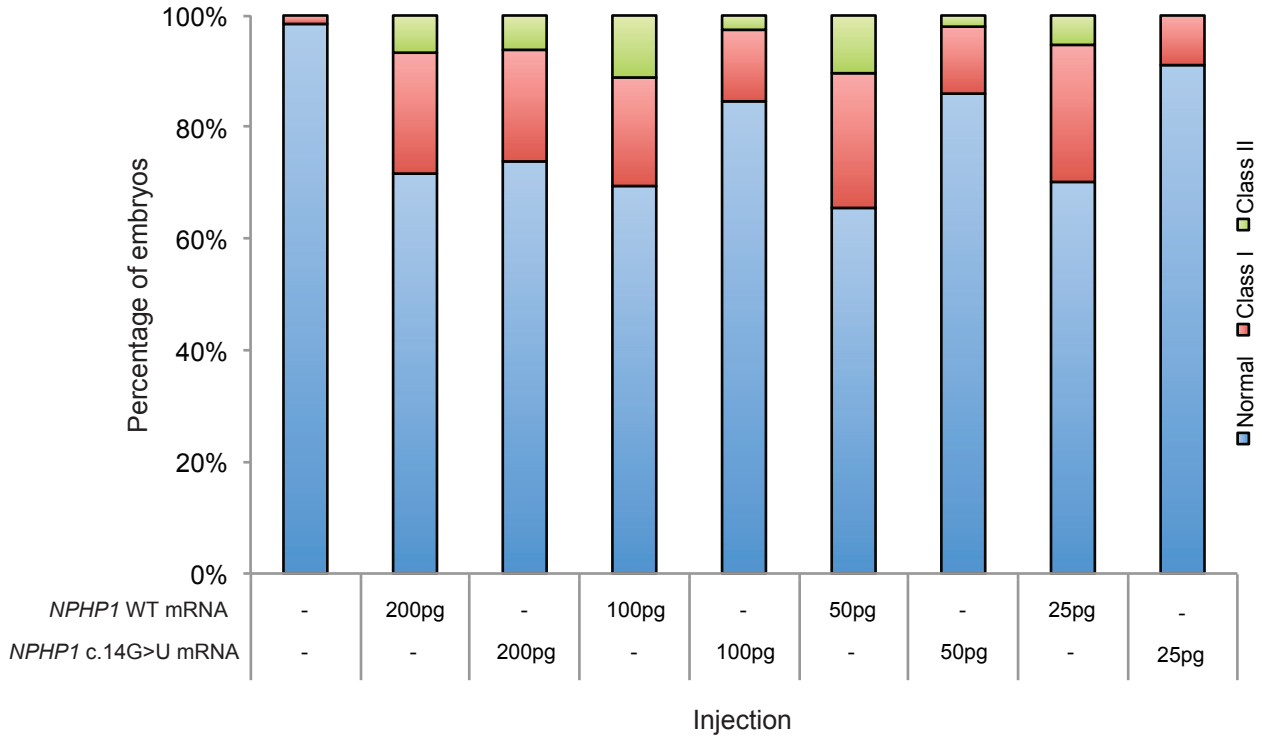

Figure S2: Dose response curve of *NPHP1* wild-type and c.14G>U mRNA.
Zebrafish embryos were injected with progressively decreasing concentrations of either wild-type (WT) or mutant (c.14G>U) human *NPHP1* mRNA and scored for gastrulation defects at the midsomite stage (see Figure 3A for representative images of each phenotypic class). WT mRNA results in a persistent, mild phenotype affecting ~30% of embryo batches; c.14G>U mRNA produces a progressive decrease in the number of affected embryos, supporting the notion that this is a loss-of-function variant (n=29-66 embryos/injection batch, repeated at least twice, with masked scoring.

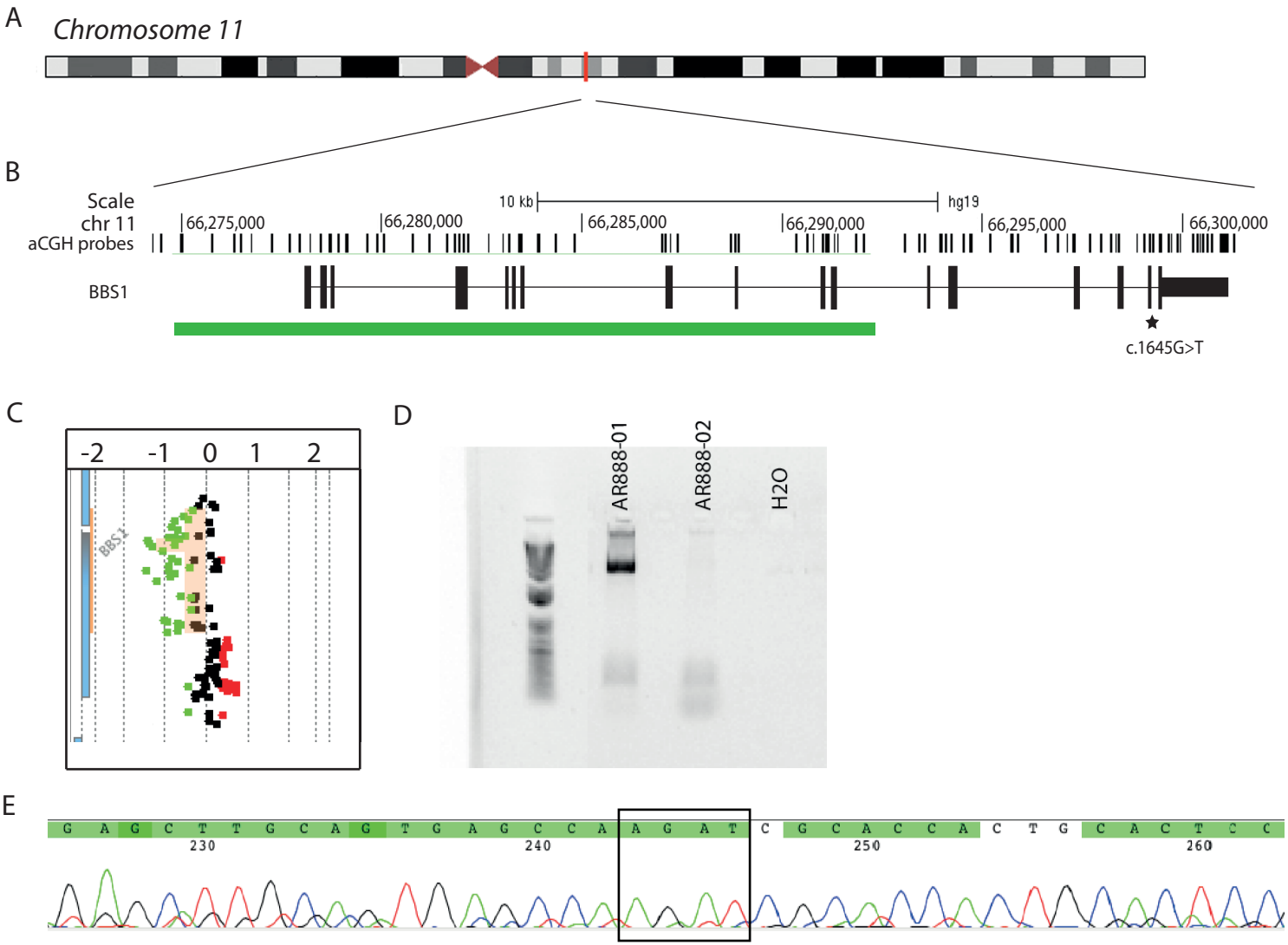

Figure S3: Characterization of the 17.7kb *BBS1* deletion in family AR888

(A) Schematic of human chromosome 11. A vertical red line indicates the position of *BBS1* (NM_024649.4) at 11q13.2.

(B) A zoomed depiction of the *BBS1* locus with a schematic illustration of exons (vertical blue bars). The genomic location on chromosome 11 (in Mb) is shown and the distribution of array comparative genomic hybridization (aCGH) probes. The solid green bar below the gene represents the genomic location of the deletion identified in AR888-03. The location of the heterozygous c.1645G>T (p.Glu549*) mutation is marked by a star.

(C) High-resolution results from the aCGH analyses in individual AR888-03 are visualized as a plot. The horizontal blue bar represents *BBS1*. Individual dots represent specific oligonucleotide probes and are indicated as black (normal copy number), red (copy number gain), and green (copy number loss) compared to a reference sample. The normalized log2 ratios of the Cy5/Cy3 intensity values for cases versus controls are shown on the Y-axis.

(D) Segregation of the *BBS1* deletion in the AR888 family. Deletion carriers are identified by clearly resolvable bands on an agarose gel electrophoresis following PCR amplification. Individual 01 harbors the deletion.

(E) Sequence traces from Sanger sequencing of the breakpoint PCR product shown in (D). A 4 bp micro-homology is present.

Table S1: Phenotypic scoring and statistical significance of interactions for zebrafish embryo injections.

In vivo complementation: Gastrulation defects scored live in midsomitic embryos							
Injection	**Normal**	**Class I**	**Class II**	**n=**	**% abnormal**	***p* vs *nphp1* MO**	***p* vs WT rescue**
nphp1 MO	27	29	4	60	55%	N/A	
nphp1 MO + *NPHP1* WT RNA	38	19	5	62	39%	0.0027	N/A
nphp1 MO + *NPHP1* c.14G>U RNA	29	20	10	59	51%	<0.0001	0.0017
nphp1 MO + *NPHP1* c.115C>A RNA	40	17	4	61	34%	0.0002	0.7126
nphp1 MO + *NPHP1* c.689C>U RNA	43	17	5	65	34%	<0.0001	0.5444
Injection	**Normal**	**Class I**	**Class II**	**n=**	**% abnormal**	***p* vs *nphp1* MO**	***p* vs WT RNA**
NPHP1 WT RNA	43	13	4	60	28%	<0.0001	N/A
NPHP1 c.14G>U RNA	48	13	4	65	26%	<0.0001	0.8842
NPHP1 c.115C>A RNA	47	12	3	62	24%	<0.0001	0.6114
NPHP1 c.689C>U RNA	41	11	4	56	27%	<0.0001	0.9697
In vivo complementation: Renal defects scored in 4 dpf larva stained with Na+/K+ ATPase antibody							
Injection	**Normal**	**Affected**		**n=**	**% abnormal**	***p* vs *nphp1* MO**	***p* vs WT rescue**
nphp1 MO	18	28		46	61%	N/A	
nphp1 MO + *NPHP1* WT RNA	32	14		46	30%	<0.0001	N/A
nphp1 MO + *NPHP1* c.14G>U RNA	24	25		49	51%	0.0403	<0.0001
nphp1 MO + *NPHP1* c.115C>A RNA	35	16		51	31%	<0.0001	0.8273
nphp1 MO + *NPHP1* c.689C>U RNA	34	17		51	33%	<0.0001	0.5127
Genetic interaction experiments: Gastrulation defects scored live in midsomitic embryos							
Morpholino target	**Normal**	**Class I**	**Class II**	**n=**	**% abnormal**	***p* vs *nphp1***	***p* vs bbs-gene**
nphp1	201	40	14	255	21%	N/A	N/A
bbs1	54	11	3	68	21%	N/A	N/A
bbs2	134	25	3	162	17%	N/A	N/A
bbs7	51	10	3	64	20%	N/A	N/A
bbs9	116	19	6	141	18%	N/A	N/A
bbs10	95	17	12	124	23%	N/A	N/A
bbs1+ nphp1	40	18	3	61	34%	0.0006	0.0005
bbs2+nphp1	89	43	16	148	40%	<0.0001	<0.0001
bbs7+nphp1	36	24	4	64	44%	<0.0001	<0.0001
bbs9+nphp1	110	41	11	162	32%	0.0248	0.0008
bbs10+nphp1	68	31	20	119	43%	<0.0001	<0.0001
Genetic interaction experiments: Renal defects scored in 4 dpf larva stained with Na+/K+ ATPase antibody							
Morpholino target	**Normal**	**Affected**		**n=**	**% abnormal**	***p* vs *nphp1***	***p* vs bbs-gene**
nphp1	70	25		95	26%	N/A	N/A
bbs1	39	16		55	29%	N/A	N/A
bbs2	35	12		47	26%	N/A	N/A
bbs7	54	10		64	16%	N/A	N/A
bbs9	13	3		16	19%	N/A	N/A
bbs10	34	11		45	24%	N/A	N/A
bbs1+ nphp1	35	25		60	42%	0.0003	0.0042
bbs2+nphp1	14	11		25	44%	<0.0001	<0.0001
bbs7+nphp1	32	24		56	43%	<0.0001	<0.0001
bbs9+nphp1	13	10		23	43%	<0.0001	<0.0001
bbs10+nphp1	31	25		56	45%	<0.0001	<0.0001

N/A=not applicable